

## Surface Structure of $\text{TiO}_2(011)-(2 \times 1)$

T. J. Beck,<sup>1</sup> Andreas Klust,<sup>1</sup> Matthias Batzill,<sup>1</sup> Ulrike Diebold,<sup>1,\*</sup> Cristiana Di Valentin,<sup>2,3</sup> and Annabella Selloni<sup>3,†</sup>

<sup>1</sup>*Department of Physics, Tulane University, New Orleans, Louisiana 70118, USA*

<sup>2</sup>*Dipartimento di Scienza dei Materiali, Universita' degli Studi di Milano-Bicocca, 20125 Milano, Italy*

<sup>3</sup>*Department of Chemistry, Princeton University, Princeton, New Jersey 08540, USA*

(Received 7 April 2004; published 16 July 2004)

A combined experimental and first principles study of the  $(2 \times 1)$ -reconstructed rutile  $\text{TiO}_2(011)$  surface is presented. Our results provide evidence that the surface structure is described by a model that includes onefold coordinated (titanyl) oxygen atoms giving rise to double bonded  $\text{Ti}=\text{O}$  species. These species should play a special role in the enhanced photocatalytic activity of the  $\text{TiO}_2(011)$  surface.

DOI: 10.1103/PhysRevLett.93.036104

PACS numbers: 68.35.Bs, 68.37.Ef, 68.43.Bc, 68.47.Gh

Titanium dioxide is a promising photocatalyst for the remediation of pollutants and the photoelectrochemical conversion of solar energy [1]. These and a wide variety of other attractive applications have stimulated a concerted effort to investigate the atomic-scale properties of  $\text{TiO}_2$  [2–5]. We present work that is motivated by the growing evidence of a dramatic face dependence in the photocatalytic activity of  $\text{TiO}_2$  [6–8]. For certain photocatalytic oxidation reactions, the  $\{011\}$  facets of polycrystalline rutile  $\text{TiO}_2$  samples are particularly active, and it has been speculated that a special atomic configuration on  $\text{TiO}_2(011)$  alters either the efficiency with which photo-generated carriers are trapped at the surface or the rate at which they are transferred at the solid-liquid interface [7]. We want to find out what this special configuration might be. In a combined experimental and theoretical study we show that the rutile  $\text{TiO}_2(011)$  surface exhibits a  $(2 \times 1)$  reconstruction and is distinct from other  $\text{TiO}_2$  surfaces by the presence of onefold coordinated (titanyl) oxygen atoms. We suggest that these species play a special role in the enhanced photocatalytic activity of the  $\text{TiO}_2(011)$  surface.

The coordination of surface atoms is a decisive factor in the surface chemistry of metal oxides [9,10]. In bulk  $\text{TiO}_2$  the titanium atoms are surrounded by octahedra of six oxygen atoms. The various crystallographic modifications of  $\text{TiO}_2$  differ in the level of distortion and the stacking sequence of these octahedra. Oxygen atoms have three Ti neighbors in all  $\text{TiO}_2$  crystal structures. Virtually all stable  $(1 \times 1)$  terminated  $\text{TiO}_2$  surfaces contain twofold coordinated O atoms and fivefold coordinated Ti atoms [2]. (This would also be the case for bulk-terminated  $\text{TiO}_2(011)-(1 \times 1)$ ; see the bottom of the model in Fig. 1.) Such undercoordinated  $\text{Ti}(5)$  atoms are preferred adsorption sites for a variety of molecules. So far, the  $\text{TiO}_2(011)$  surface has been investigated only in a somewhat indirect fashion. Based on an early low-energy electron diffraction (LEED) study [11], it was concluded that  $\text{TiO}_2(001)$  forms  $(011)-(2 \times 1)$  oriented facets upon annealing to intermediate temperatures. While the surface chemistry of such “ $(011)$ -faceted”  $\text{TiO}_2$  has been

thoroughly tested with a large variety of organic molecules [9] and exhibits a high photocatalytic activity [12], the specific details on the arrangement and coordination of surface atoms is not known.

All experiments in this work were performed in ultra-high vacuum at a base pressure of  $1 \times 10^{-10}$  mbar. Polished  $\text{TiO}_2(011)$  samples were cleaned by sputtering and subsequent annealing in the range of 500–850 °C. Cleanliness of the surface was checked by low-energy  $\text{He}^+$  ion scattering. Empty-states scanning tunneling microscopy (STM) images were acquired with positive sample bias voltages. During STM, the sample was held close to room temperature. Photoemission measurements were performed at the Center for Advanced Microstructures and Devices (CAMD) on the 3m-TGM and the PGM beam lines.

LEED indicates a  $(2 \times 1)$  reconstruction with the  $(0, \frac{1}{2})$  superstructure spots along the  $[100]$  direction (see inset of Fig. 2). This reconstruction was observed up to the highest annealing temperatures achievable in the experimental setup (850 °C). The  $(2n-1, 0)$  spots were absent for all electron energies consistent with the glide plane symmetry present in the bulk  $\text{TiO}_2$  structure. This glide plane symmetry is maintained by our model of the surface

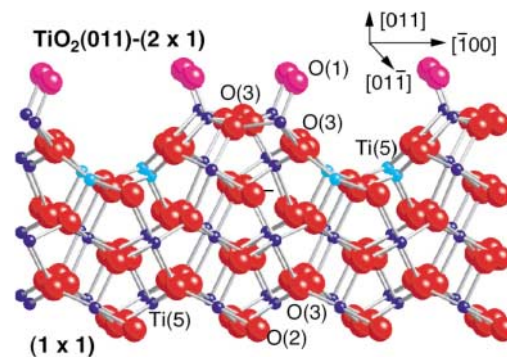


FIG. 1 (color online). Model of a  $\text{TiO}_2(011)$  surface. The top of the slab shows the proposed geometry of the  $(2 \times 1)$  reconstruction; the bottom shows the bulk-terminated  $(1 \times 1)$  surface. The coordination of surface atoms is indicated.

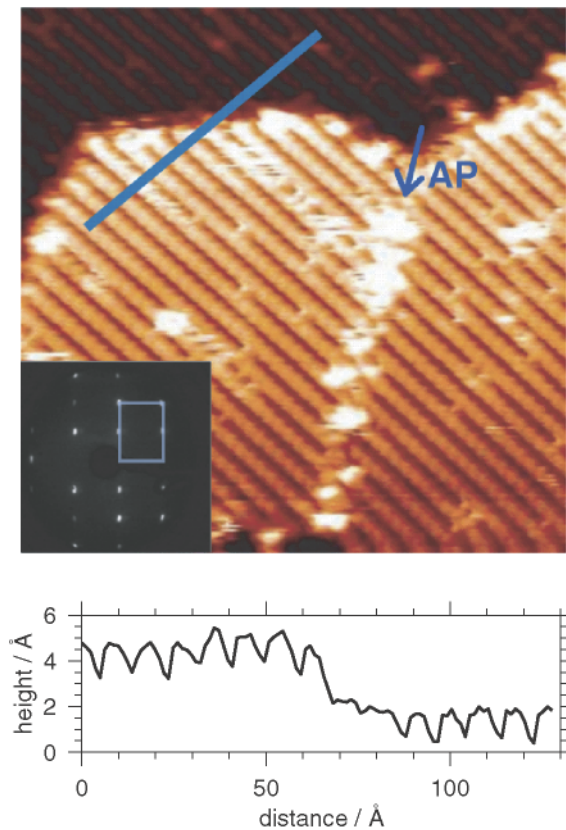


FIG. 2 (color online). Empty state STM image ( $220 \text{ \AA} \times 220 \text{ \AA}$ ) of a  $\text{TiO}_2(011)-(2 \times 1)$  surface. AP marks an antiphase domain boundary. The line profile in  $[100]$  direction along the line marked in the STM image is shown in the lower graph. The inset shows the LEED pattern of the surface with a rectangle denoting the  $(1 \times 1)$  unit cell.

reconstruction. STM shows surfaces with wide terraces separated by single-layer height steps (Fig. 2). STM shows alternating dark and bright rows along the  $[0\bar{1}1]$  direction, with a periodicity of  $9 \text{ \AA}$  and an apparent corrugation of  $2 \text{ \AA}$  across these rows. For lower annealing temperatures, antiphase domain boundaries are occasionally visible; one of them is marked AP in Fig. 2.

Interestingly, the  $\text{TiO}_2(011)-(2 \times 1)$  surface investigated here is fully oxidized under typical preparation conditions. Displayed in Fig. 3 are photoemission spectra of the valence band region. Results from  $\text{TiO}_2(110)-(1 \times 1)$  and  $\text{TiO}_2(011)-(1 \times 2)$  samples are shown for comparison. The upper set of spectra was taken at  $48 \text{ eV}$ , where Ti-derived states are emphasized by resonant photoemission effects [2]. On rutile  $(110)-(1 \times 1)$ , a few percent of the “bridging” O(2) atoms can be easily removed by annealing *in vacuo* and give rise to a defect state in the  $3 \text{ eV}$  band gap (see arrow in Fig. 3). These point defects play a special role in adsorption processes [3–5]. Applying exactly the same preparation conditions to  $\text{TiO}_2(011)-(1 \times 2)$  does not result in a defect state, indicating a stoichiometric surface.

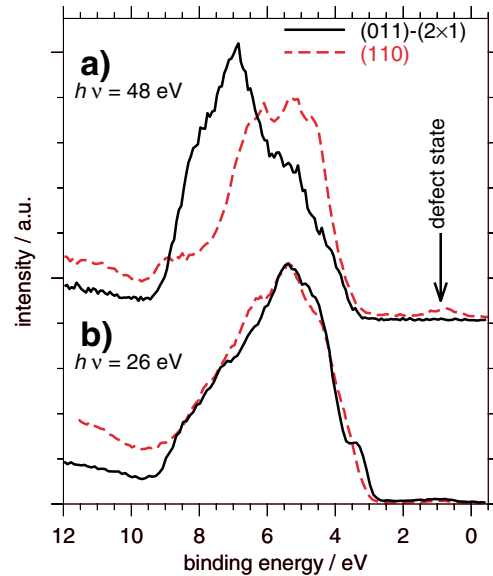


FIG. 3 (color online). Photoemission spectra of the valence band of  $\text{TiO}_2(011)-(2 \times 1)$  (solid lines) and  $\text{TiO}_2(110)$  (dashed lines) for two different photon energies:  $h\nu = 48 \text{ eV}$  (a) and  $26 \text{ eV}$  (b). The energy zero is at the Fermi energy.

In the attempt to find a structural model capable to explain the experimental observations, we performed density functional theory calculations within the Car-Parrinello approach [13,14], using the Perdew-Burke-Ernzerhof [15] exchange-correlation functional and ultrasoft pseudopotentials [16], together with a plane-wave expansion of the Kohn-Sham orbitals. Slab models with both four and six Ti layers were used. The supercell comprised two  $2 \times 1$  surface cells corresponding to a surface area of  $9.27 \times 11.00 \text{ \AA}^2$  (the theoretically optimized bulk lattice parameters were taken from Ref. [17]). All atoms in the upper three or five layers (in the case of the four and six layer slab, respectively) were relaxed using a second-order damped dynamics until the residual forces were less than  $0.025 \text{ eV/\AA}$ , whereas the atoms in the lowest layer were kept fixed in their bulk positions. The use of a thicker slab was found important for the calculation of surface energies, for which we followed the procedure described in Ref. [18].

Many different initial geometries were constructed and optimized, with either stoichiometric or partially reduced surfaces. All resulting structures were found to have surface energies larger than the relaxed unreconstructed slab, with the single exception of the model shown in Fig. 1. Besides being more favorable than the nonreconstructed surface, this model was also found to be extremely robust with respect to either simulated annealing treatments or change of the initial starting geometry for the optimization procedure. The  $(2 \times 1)$  structure in Fig. 1 is perfectly stoichiometric and its main characteristic is the presence of onefold coordinated oxygen atoms, O(1), with corresponding Ti—O(1) bond distances of

1.62 Å. Such bond-lengths are  $\sim 0.3$  Å shorter than typical Ti—O bonds, and essentially correspond to Ti=O double bonds (denoted Ti=O in the following). Although no Ti=O species have been so far reported on TiO<sub>2</sub> surfaces, Ti=O is known to occur in a variety of Ti(IV)-containing compounds, such as complex oxides and titanosilicate materials [19,20], as well as at the edges of TiO<sub>2</sub> nanoparticles [21], and are usually associated to a square-pyramidal coordination environment of Ti atoms, similar to that of the topmost Ti atoms in Fig. 1. The titanyl O(1) atoms form zig-zag surface chains along the  $[0\bar{1}1]$  direction, and, between different chains along the  $[0\bar{1}1]$  direction, wide “valleys” exposing fivefold coordinated Ti atoms, Ti(5), are present. All other surface atoms are fully coordinated.

The electronic density of states (DOS) for the Ti=O double bond model is shown in Fig. 4, where it is compared to an analogous calculation for the TiO<sub>2</sub>(110) surface [22]. The most relevant difference between the two calculated curves is at the upper edge of the O(2p) valence band, where a well-defined peak is present for the (011) surface, originating from the O(1) titanyl atoms (see arrow in Fig. 4). Comparison of this theoretical result with experiment is not straightforward due to the strong dependence of the photoemission spectra on the photon energy  $h\nu$ . It is, however, remarkable that a pronounced shoulder at the upper edge of the O(2p) band is seen for the TiO<sub>2</sub>(011)-(2 × 1) surface but not for the TiO<sub>2</sub>(110) one at  $h\nu = 26$  eV [see Fig. 3(b)].

Several experimental observations give additional credibility to the proposed model. First, high-resolution STM (Fig. 5) shows that the rows consist of bright spots, arranged in a zig-zag pattern. The calculated empty-state image [22,23] agrees very well with experimental results. Interestingly, the bright spots correspond to the position of the titanyl groups; this is at variance with analogous

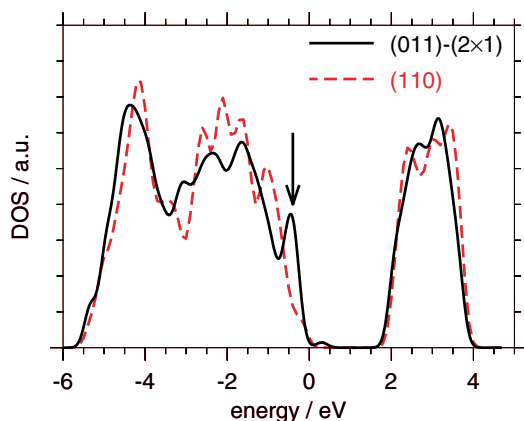


FIG. 4 (color online). Calculated valence and conduction band DOS of TiO<sub>2</sub>(011)-(2 × 1) (solid lines) and TiO<sub>2</sub>(110) (dashed lines). The energy zero is at the upper edge of the valence band. The tiny feature just above  $E = 0$  is related to the fixed atoms on the lower surface of the slab.

images for other TiO<sub>2</sub> surfaces where typically the Ti(5) atoms are seen in empty-states STM images [24]. This difference can be attributed to the fact that on the (011) surface the outermost Ti atoms are chemically/coordinatively saturated so that the geometrical effects [highly protruding O(1) atoms] become dominant.

Second, the position of adsorbates is compatible with the model displayed in Fig. 1. We exposed the surface to formic acid (HCOOH), which is a well-established test molecule for probing Lewis acid/base adsorption reactions on TiO<sub>2</sub> surfaces [2]. The undercoordinated Ti(5) atoms in the valleys act as Lewis-acid sites, whereas the strongly bound O(1) atoms and the threefold coordinated O atoms on top of the rows are expected to block adsorption. The dosage of small amounts of HCOOH at room temperature induces bright protrusions in STM (labeled F in Fig. 6). The exact bonding geometry of formic acid on TiO<sub>2</sub>(011)-(1 × 2) will be the topic of a future paper; here it is noteworthy that adsorbate-induced features are clearly located *between* the rows, in agreement with the position of the Ti(5) sites in the model. Third, the observation that TiO<sub>2</sub>(011)-(2 × 1) is hard to reduce (Fig. 3) is also in-line with the proposed model. The Ti=O double bonds formed by the surface O(1) atoms are hard to break by simply heating the sample.

The Ti=O species on TiO<sub>2</sub>(011)-(2 × 1) distinguish this system from all the other single-crystalline TiO<sub>2</sub> surfaces that have been characterized so far. It is thus suggestive that they may play a major role in the enhanced photocatalytic activity of this face. The photocatalytic process starts with the excitation of an electron-hole pair across the band gap. These electrons/holes may migrate to the surface where, in the simplest picture, they may reduce/oxidize different adsorbed species [1]. The electron and hole recombine with a high probability,

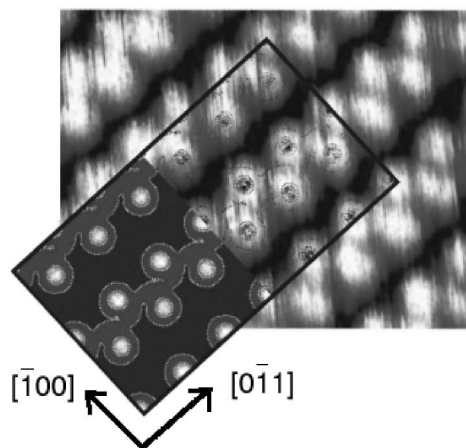


FIG. 5. High-resolution STM image ( $40 \text{ \AA} \times 30 \text{ \AA}$ ) of TiO<sub>2</sub>(011)-(2 × 1). The overlay shows contours of the local density of states in a plane 2.2 Å above the outermost Ti atoms, calculated by integrating the electronic states within a  $\sim 2$  eV window from the conduction band edge.



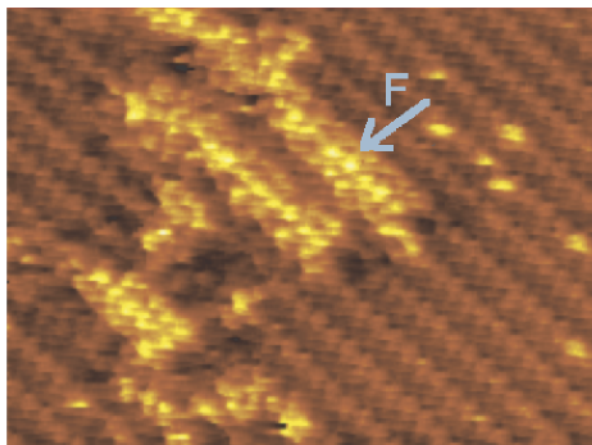


FIG. 6 (color online). STM image ( $140 \text{ \AA} \times 100 \text{ \AA}$ ) of a  $\text{TiO}_2(011)-(2 \times 1)$  surface exposed to 10 L [1 langmuir (L) =  $10^{-6}$  Torr s] of formic acid at room temperature.

however, which makes the process rather inefficient. “Surface trapping sites” increase the lifetime of the electron/hole, and it is probable that either the  $\text{Ti}=\text{O}$  species themselves, or a molecule that is strongly bound at such a site [21], act as efficient trapping sites. As a matter of fact, our calculations indicate that the states at the upper edge of the valence band are localized at the surface O(1) atoms (see Fig. 4). Therefore these atoms should be able to efficiently trap the photogenerated holes and readily oxidize acceptor species present on the surface.

With this Letter we have shown how to prepare a well-characterized surface with a high coverage of titanyl groups. This is an important first step for applying surface science techniques that are capable of unravelling reaction mechanisms with the high level of detail that is needed in order to thoroughly understand the special role these species may play in (photo)catalytic processes.

This work was supported by NSF Grants No. CHE-0109804 and No. CHE-0121432 and by NASA-EPSCoR. We thank Yaroslav Losovyj (CAMD) for help with the photoemission experiments and E. L. D. Hebenstreit for photoemission spectra of the  $\text{TiO}_2(110)$  surface. The calculations were performed at the Pittsburgh Supercomputer Center and at the Keck Computational Materials Science Laboratory of Princeton University.

\*Electronic address: diebold@tulane.edu

†Electronic address: aselloni@princeton.edu

- [1] A. L. Linsebigler, G. Lu, and J. T. Yates, Jr., *Chem. Rev.* **95**, 735 (1995).
- [2] U. Diebold, *Surf. Sci. Rep.* **48**, 53 (2003).
- [3] R. Schaub, P. Thostrup, N. Lopez, E. Laegsgaard, I. Stensgaard, J. K. Nørskov, and F. Besenbacher, *Phys. Rev. Lett.* **87**, 266104 (2001).
- [4] I. M. Brookes, C. A. Muryn, and G. Thornton, *Phys. Rev. Lett.* **87**, 266103 (2001).
- [5] R. Schaub, E. Wahlstroem, A. Ronnau, E. Laegsgaard, I. Stensgaard, and F. Besenbacher, *Science* **299**, 377 (2003).
- [6] P. A. M. Hotsenpiller, J. D. Bolt, W. E. Farneth, J. B. Lowekamp, and G. S. Rohrer, *J. Phys. Chem. B* **102**, 3216 (1998).
- [7] G. S. Rohrer, in *Oxide Surfaces*, edited by D. P. Woodruff, *The Chemical Physics of Solid Surfaces Vol. 9* (Elsevier, Amsterdam, 2001), Chap. 12, p. 485
- [8] T. Ohno, K. Sarukawa, and M. Matsumura, *New J. Chem.* **26**, 1167 (2002).
- [9] M. A. Barteau, *Chem. Rev.* **96**, 1413 (1996).
- [10] C. Noguera, *Physics and Chemistry of Oxide Surfaces* (Cambridge University Press, Cambridge, 1996).
- [11] L. E. Firment, *Surf. Sci.* **116**, 205 (1982).
- [12] J. N. Wilson and H. Idriss, *J. Catalysis* **214**, 46 (2003).
- [13] R. Car and M. Parrinello, *Phys. Rev. Lett.* **55**, 2471 (1985).
- [14] K. Laasonen, A. Pasquarello, R. Car, C. Lee, and D. Vanderbilt, *Phys. Rev. B* **47**, 10142 (1993).
- [15] J. P. Perdew, K. Burke, and M. Ernzerhof, *Phys. Rev. Lett.* **77**, 3865 (1996).
- [16] D. Vanderbilt, *Phys. Rev. B* **41**, 7892 (1990).
- [17] M. Lazzeri, A. Vittadini, and A. Selloni, *Phys. Rev. B* **63**, 155409 (2001).
- [18] V. Fiorentini and M. Methfessel, *J. Phys. Condens. Matter* **8**, 6525 (1996).
- [19] F. Farges, G. E. Brown, Jr., and J. J. Rehr, *Phys. Rev. B* **56**, 1809 (1997).
- [20] M. A. Roberts, G. Sankar, J. M. Thomas, R. H. Jones, H. Du, J. Chen, W. Pang, and R. Xu, *Nature (London)* **381**, 401 (1996).
- [21] T. Rajh, J. M. Nedeljkovic, L. X. Chen, O. Poluetkov, and M. C. Thurnauer, *J. Phys. Chem. B* **103**, 3515 (1999); P. C. Redfern, P. Zapol, L. A. Curtiss, T. Rajh, and M. C. Thurnauer, *J. Phys. Chem. B* **107**, 11419 (2003).
- [22] Both the DOS (Fig. 4) and the STM image (Fig. 5) have been computed using the PWSCF code by S. Baroni, S. de Gironcoli, A. dal Corso, and P. Giannozzi, which is available at <http://www.pwscf.org>.
- [23] J. Tersoff and D. R. Hamann, *Phys. Rev. Lett.* **50**, 1998 (1983).
- [24] U. Diebold, J. F. Anderson, K. O. Ng, and D. Vanderbilt, *Phys. Rev. Lett.* **77**, 1322 (1996).